Orientational defects on a hydrogen-bonded chain

R. Mittal and I. A. Howard
Department of Physics, University of Texas at Arlington, Arlington, Texas 76019
(Received 21 July 1995; revised manuscript received 20 February 1996)

In hydrogen-bonded crystals such as ice, it has been proposed that charge transport occurs through a process involving two types of defects (the so-called orientational and ionic defects) in the proton sublattice. We have investigated the formation and dynamics of the orientational defects through two approaches: a quantum-chemical study of the barrier to rotation in finite chains of H_2O molecules, and a study, based on an extended tight-binding model, of the formation and motion of these defects. We find from the first part of this study that the barrier to rotation may be nearly an order of magnitude lower than the barrier to proton hopping along the chain. The subsequent construction of the modified tight-binding model allows us to simulate motion in a uniform electric field of a pair of (charged) orientational defects. Calculated mobilities for the more mobile positively charged defect are in the range 0.39–0.46 $cm^2/V\,s$ for a dielectric screening constant of 50, in agreement with available experimental values. [S0163-1829(96)01022-3]

I. INTRODUCTION

Hydrogen bonding is of prime importance in a wide variety of systems, ranging from biological materials to some ferroelectrics.[1] The mechanisms involved in the dynamics of charge transport in such systems have been the subject of much recent study. The prototypical materials studied have been either the hydrogen halides[1–4] or ice.[1,5] It has long been accepted that in water, and even more so in ice, the hydroxyl (OH^-) and hydroxonium (H_3O^+) ions propagate with mobilities far in excess of those reported for any other ions. Eigen and De Maeyer[6] reported, for instance, a mobility of $\ll 10^{-8}$ $cm^2/V\,s$ for the Li^+ ion in ice, while the mobilities of protons in ice were found to be between 0.1–0.5 $cm^2/V\,s$. The latter mobilities are comparable to those of electrons in a semiconductor such as TiO_2. Ice is of course electronically an insulator (with band gap $\sim$14 eV, based on our short-chain Hartree-Fock calculations as described in the Results section); the mechanisms of such rapid ionic charge transport are of obvious interest.

A single chain of molecules in a material such as ice is shown schematically in Fig. 1. There are obviously two degenerate ground-state phases of such a chain: one in which covalent bonds link the backbone hydrogens with the oxygens on their left, and one in which they link to the right. It is believed that two types of chain defects are responsible for the observed protonic transport: the ionic, or hopping, defect, and the orientational defect (also called the Bjerrum defect[7]). Each type of defect can be thought of as a domain wall mediating the transition from one ground-state phase to the other. The ionic defect involves the displacement of protons from one energetic minimum to the other between two oxygen atoms along the backbone. A pair of ionic defects is shown in Fig. 2(a); it is evident that the leftmost will be positively charged and constitute an H_3O^+ ionic group, while the rightmost is negative and is effectively an OH^-. The orientational defect, the subject of this study, involves a rotation of H_2O units from one orientational energetic minimum to another, with the O-H covalent bond off the backbone ''replacing'' the one along the backbone, or vice versa. A pair of charged orientational defects is shown in Fig. 2(b). The charges associated with the orientational defects are more clearly illustrated in Fig. 2(c). Proton transport is postulated to take place through sequential propagation of an ionic and an orientational defect, after which the chain is restored to its initial configuration and free to conduct a subsequent injected proton.

A number of one-dimensional phenomenological models[8–13] have been constructed to explain proton motion via the hopping defect in a hydrogen-bonded crystal. In addition, attempts have been made to model phenomenologically the combined hopping and rotational motion necessary for sustained proton transport in a crystal such as ice.[14–17] Although the physical ice crystal is obviously not one-dimensional, the defect propagation process proceeds along a path (a so-called Bernal-Fowler filament[18]) which can be effectively modeled as one-dimensional. In the phenomenological studies mentioned, the defects are modeled as solitonic modulations of the proton displacement pattern. In this paper, we carry out a two-part study of orientational defects, using ice as our prototypical material; the first part deals with the relative height of energetic barriers to hopping and to rotation in a finite chain of H_2O molecules, while in the second part we develop a model of the dynamics of motion of the orientational defects, incorporating a classical lattice and a quantum-mechanical electronic system with electron-lattice coupling.

II. METHODS

We have used two approaches to study the formation and dynamics of orientational defects in a hydrogen-bonded

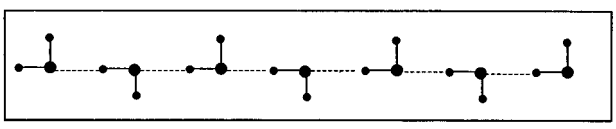

FIG. 1. Schematic representation of a chain of molecules in a crystal of ice. Large circles are oxygens, small circles hydrogens.

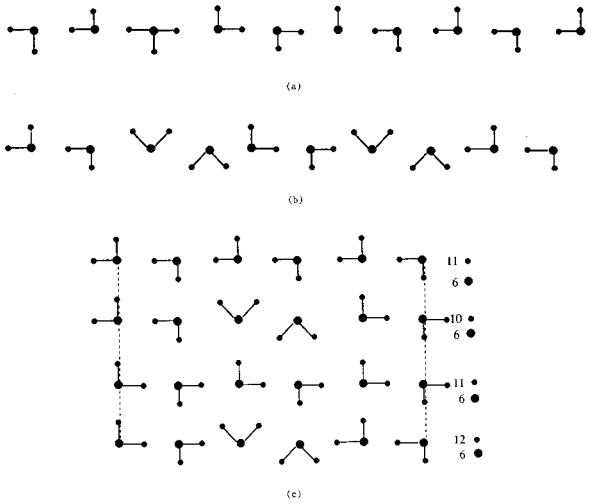

FIG. 2. A pair of ionic (a) and orientational (b) defects in a chain of H_2O molecules. In (c), the charges associated with the orientational defects are depicted. Here the first and third panels show a section of chain in the ground state, while the second shows a chain containing a negative defect (ten protons, six oxygens between the dashed lines) and the fourth, a chain with a positive defect (12 protons, six oxygens between dashed lines).

chain. The first involved a set of *ab initio* Hartree-Fock quantum-chemical calculations on a chain of five hydrogen-bonded H_2O molecules in a configuration corresponding to that of a Bernal-Fowler filament[18] in ice. On this chain, we have carried out a series of calculations to estimate the height of the double-well energy barrier associated with formation of the orientational defect. Since both ionic and orientational defects can exist in such chains, we have also estimated, for comparison, the height of the double-well barrier for the formation of the ionic defect. The calculations were performed using the GAUSSIAN 92 package.[19] Both the 6-31G* and 6-311G* bases were used for comparison, and calculations were performed both at the unrestricted Hartree-Fock (UHF) and fourth-order Moller-Plesset (MP4) levels,[20] the latter constituting a perturbative estimate of correlation effects. The 6-31G* basis was initially chosen as a result of the observation of Hehre *et al.*[20] that this basis adequately predicted optimal geometry for the isolated H_2O molecule. Bonding was assumed to be tetrahedral, as in the cubic I_c phase of ice;[21] the oxygen-oxygen distance accordingly was taken to be 2.7497 Å. The initial calculation involved estimating the barrier to proton hopping along the chain, as opposed to rotation of an H_2O unit. This was accomplished by stepping the displacement of all the ''backbone'' protons simultaneously along the chain. This was followed by an estimate of the rotational barrier, carried out by simultaneously rotating each H_2O unit. Finally, to estimate the effects of interchain interaction, we considered two parallel chains, hydrogen-bonded as in an ice crystal, and carried out a simultaneous rotation of all H_2O units on one chain only. Neither the hopping process nor the rotational process, of course, proceeds physically through simultaneous displacement of all units along a chain. In the phenomenological models cited above, the proton potential is usually written as a sum of a double-well potential and a set of harmonic terms coupling displacements of nearest-neighbor on-chain protons. Our calculations allow us to evaluate the double-well part of the proton potential; for the rotational case, the calculated barrier height will then be compared with that originating from the tight-binding dynamical calculations that follow. Results of the initial set of quantum-chemical calculations are presented in Sec. III A.

In the second approach to the problem, we constructed a model for the formation and dynamics of orientational defects in a chain of 100 H_2O units, under circular boundary conditions. This was based on a Hamiltonian (to be described below in more detail) consisting of the sum of classical lattice terms and electronic terms arising from a modified tight-binding model. (We note that Springborg[3] has used a model similar in some respects to ours in his discussion of ionic defects in HF.) The electronic Hamiltonian contained off-diagonal terms incorporating an angle-dependent transfer integral for each of the four occupied valence bands of ice, and diagonal terms which included the angle-dependent effects of Coulomb interactions between an electron on a given lattice site and the net charges on atoms in adjacent units. Calculation of the dynamics then involved specifying the initial angular configuration of the lattice, diagonalizing the resulting electronic Hamiltonian, and using the resulting eigenvectors to solve the lattice equations of motion (containing coupled electron-lattice force terms) for a short time step. The resulting lattice configuration was then used to construct a new electronic Hamiltonian, and so forth. This approach yielded angular displacements and velocities of the lattice H_2O units; electronic eigenfunctions, one-electron energies, and total energy, as a function of time. Imposition of a uniform electric field was subsequently carried out by addition of terms linear in field strength to the diagonal elements of the Hamiltonian. For simplicity, the chain was ''linearized'' to be two-dimensional, so that the H-O-H bond angle in a single unit was 90°.

We now describe in more detail this second approach and its parametrization. The lattice Hamiltonian was simply the sum of Coulomb repulsions between all ionic cores on a given site (a site being an H_2O unit) and all those on its nearest-neighbor and some next-nearest-neighbor sites. The charge associated with a core was taken to be $+6|e|$ for oxygen and $+1|e|$ for hydrogen. In the simulations of motion in the presence of a field, these interactions were modified by different dielectric screening constants to vary the barrier height in the double-well potential. The static dielectric constant of ice is large; Bernal and Fowler[18] quote it as ~88. However, over the interaction distances of concern here, it is probably not reasonable to expect the full screening to apply; we tried screening constants between 1 and 100.

The electronic Hamiltonian used in the absence of the field can be written as

$$H_{\mathrm{el}}=\sum_{i=1}^{4}\sum_{s=1}^{2}\sum_{n=1}^{100}\left[-t^{i}_{n+1,n}\left(c^{i+}_{n,s}c^{i}_{n+1,s}+c^{i+}_{n+1,s}c^{i}_{n,s}\right)\right.$$
$$\left.+f(n+1,n,n-1)c^{i+}_{n,s}c^{i}_{n,s}\right], \qquad (1)$$

where the index i sums over the four occupied valence bands of the crystal, s sums over spins, and n sums over lattice sites (H_2O units). The transfer integral is $t^{i}_{n+1,n}$, and

$f(n+1,n,n-1)$ is the modification of site energy on site n due to the angular displacement of sites $n+1$, n, and $n-1$. The transfer integral is a function of the angular displacement of adjacent lattice sites; we have parametrized it using the results of the GAUSSIAN 92 runs described above. The width W^i of each of the occupied valence bands ($W^i=4t^i$) was calculated as a function of the simultaneous angle of rotation of all the sites, and the bandwidths were then fitted to a function of the form

$$W^i=4t^i_{n,n+1}=A^i\cos(2\theta_n+2\theta_{n+1})+B^i \tag{2}$$

with A^i and B^i constants and θ_n the angular displacement of site n. In Eq. (1), the function $f(n+1,n,n-1)$ measured the change in energy of an electron on site n due to Coulomb interactions between the electron (assumed, due to the electronegativity of oxygen, to effectively sit at the position of the oxygen atom) and adjacent atoms, taken out to next-nearest-neighbor atoms. Therefore f was a function of the rotational angles of the units n, $n+1$ and $n-1$. The adjacent atoms were taken to have fixed net charges given by the average Mulliken charges for that atom type from the GAUSSIAN 92 finite chain results at the energy minima. In the cases where screening was applied to the core-core repulsions, it was also applied here.

The equations of motion for the lattice sites included the Coulomb forces resulting from the core-core interactions, the electron-lattice forces computed from the negative gradient of the expectation value of the electronic Hamiltonian, and a phenomenological damping term proportional to the site angular velocity. All O-H bond lengths were held constant, so that rotational motion only was allowed. The equations of motion were solved at each iteration for a time step of 10^{-15} s, well below the time interval ($\sim 2.6\times10^{-14}$ s) associated with the zone-center optical mode of the lattice. Most of the results presented in this paper were generated using simple Euler integration for the equations of motion; use of the fourth-order Runge-Kutta technique[22] gave rise to minimal changes in most results of interest, while greatly increasing computational time.

A pair of orientational defects was added to the chain by modulating the proton displacement pattern with two hyperbolic tangent functions, one centered at site 30, and the other at site 70. Thus the chain ends were both in the same phase of rotational displacement, corresponding to one of the degenerate ground states, while the central section was in the phase corresponding to the other minimum. The displacement pattern so constructed was then allowed to relax under the operation of the equations of motion.

Simulation of motion in a uniform electric field was accomplished, as mentioned above, by the addition of a set of terms

$$\sum_{n=1}^{100}(n-1)(|e|E_o a)c_n^+ c_n \tag{3}$$

(where n is site number, e is the electronic charge, E_o is the field strength, and a is the intersite distance 2.7497 Å) to the electronic Hamiltonian, and addition of the appropriate terms to the equations of motion to represent torque exerted by the field on the rigid H_2O unit. Results of calculations carried out with this model of the chain dynamics are presented in Sec. III B.

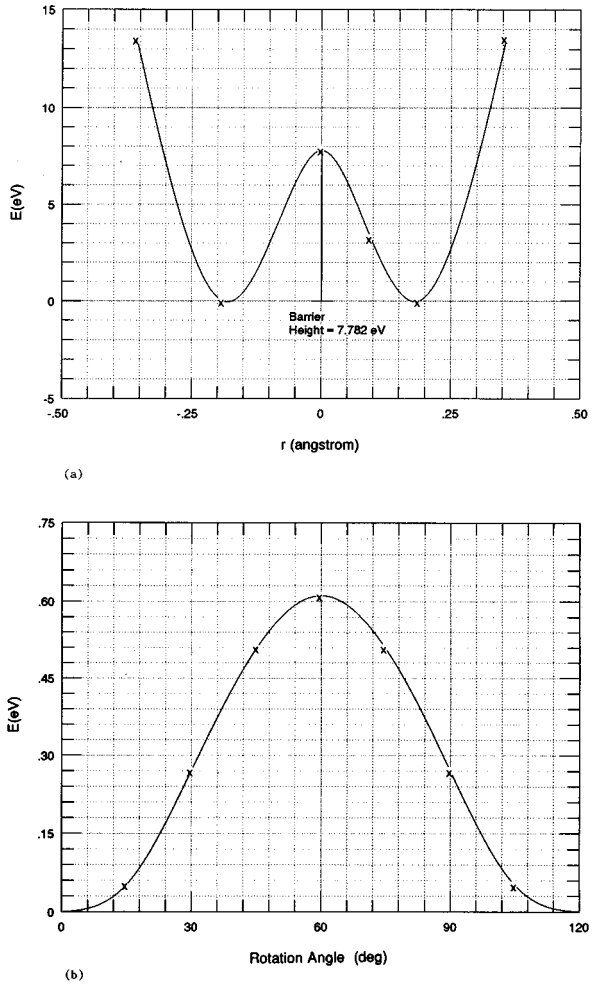

FIG. 3. (a) Total energy versus simultaneous proton displacement along the backbone and (b) total energy versus simultaneous angular displacement of H_2O units, for a chain of five molecules as described in the text. The solid line represents a fit to the data resulting from UHF calculations with a 6-31G* basis; the zero of displacement represents the midpoint between oxygens in (a); rotational angle in (b) is the projection onto two dimensions.

III. RESULTS

A. Quantum-chemical calculations

In the initial set of unrestricted Hartree-Fock calculations on the five-site chain, the backbone protons were simultaneously stepped from left to right along the direction between two oxygens to get an estimate of the hopping barrier. Figure 3(a) shows the plot of total energy versus hydrogen position at the UHF level. A double-well barrier in total energy of 7.78 eV, or 1.51 eV/site if the barrier is considered on a ''per site'' basis, was found using the 6-31G* basis. Including MP4 correlation corrections with the same basis, we found barrier height decreased to 5.15 eV or 1.03 eV/site.

The rotational double-well barrier, found by simultaneously rotating each H_2O unit in the finite chain, was found to be 0.12 eV/site, an order of magnitude smaller than the hopping barrier. Figure 3(b) shows the total energy versus rotational angle using the basis set 6-31G*. The rotational barrier was unaffected, to within a hundredth of an electron

volt, by using the larger 6-311G** basis set or by applying MP4 correlation corrections. In the case of the parallel chain model, the rotational barrier increased to 0.20 eV/site at the UHF level with the 6-31G* basis. This is to be expected, since for a H_2O molecule to rotate in this case, it is necessary that it break the hydrogen bond with the connected parallel chain. Although the rotational barrier is higher in the latter case, it is still considerably smaller than the hopping barrier.

The bandwidths of the four valence ''bands'' for our five-site chain as a function of angle were computed and the result for each valence band was separately fitted to the functional form of Eq. (2) in Sec. II; the results were used to parameterize the off-diagonal terms of the electronic Hamiltonian.

B. Dynamical model

We first tested the tight-binding dynamical model to be certain that it reproduced the rotational double-well potential. In doing this, we bypassed the equations of motion and calculated the total energy during a sequential series of simultaneous rotations of all the rigid H_2O units, as in the finite-chain runs. Results for the lattice energy, total electronic energy, and total energy are seen in Fig. 4. Using a screening factor of one, we found the rotational barrier to be 0.14 eV/site, which compares very nicely to the 0.12 eV/site barrier found from the short-chain quantum-chemical calculations. We next allowed the equations of motion to operate, and released the lattice from various initial nonequilibrium configurations. The lattice always returned to the nearest total-energy minimum, as expected. Thus the lattice is stable within this model in both of the two degenerate ground-state phases of angular displacement, which we have labeled the 0° phase and the ±90° phase.

We next formed orientational defects, as described above, centered at sites 30 and 70, using a hyperbolic tangent envelope function for the proton displacement pattern in the vicinity of the defects. Figure 5 shows the angular site displacement and site velocity as a function of site number and time for a case where the screening is 100, with a damping constant of 10^{-15} eV s. This plot is based on an initial hyperbolic tangent envelope with a characteristic width of two sites. These solitonic defects were stable, as can be observed from the declining velocity over 5000 iterations. From the displacement plot we see that in the final configuration, the sites between 30 and 70 are sitting in the ±90° phase, while all other sites remain in the 0° configuration. We tested a number of different values of initial soliton width, from two sites to ten sites. In all these cases, the soliton tended toward a two-site width as we let the lattice relax in time. The stability of very narrow solitons in our model casts doubt on the validity of a continuum model for proton transfer in similar hydrogen bonded chains. In the remainder of our calculations, we began with a two-site-wide soliton. We found the soliton formation energy (taken as the difference in total energy of the chain with and without a defect pair) to be approximately 0.05 eV/pair with a screening of 100. The formation energy increased linearly with decreasing screening, however.

A uniform electric field was then applied to a stable defect pair. Figure 6 shows the rotational site displacement and site angular velocity for an electric field of 436 kV/cm, a screening factor of 100, and a damping of 10^{-15} eV s. We note that the defect on the right (the positive defect), moves toward the right (in the field direction), while the defect on the left, the negative defect, moves to the left. Within 5 ps (5000 iterations) the two defects collide and recombine. The proton rotational displacement pattern ultimately stabilizes in a configuration such that the sites between one and 30, and those between 70 and 100, are in a phase with alternating displacements approaching ±3 rad (~±180°), while the central portion of the chain remains in the ±90° phase. We had expected that the initial central phase of ±90° displacement

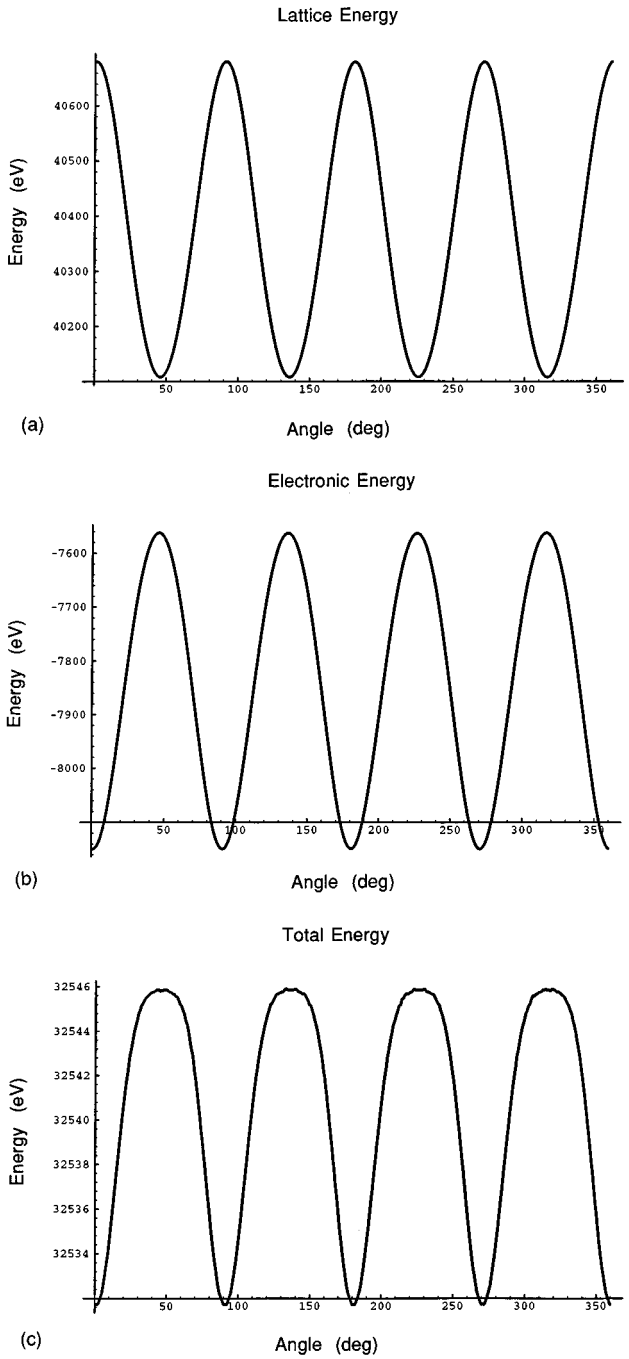

FIG. 4. Lattice energy (a), electronic energy (b) and total energy (c) of the 100-site chain as a function of simultaneous site rotational angle.

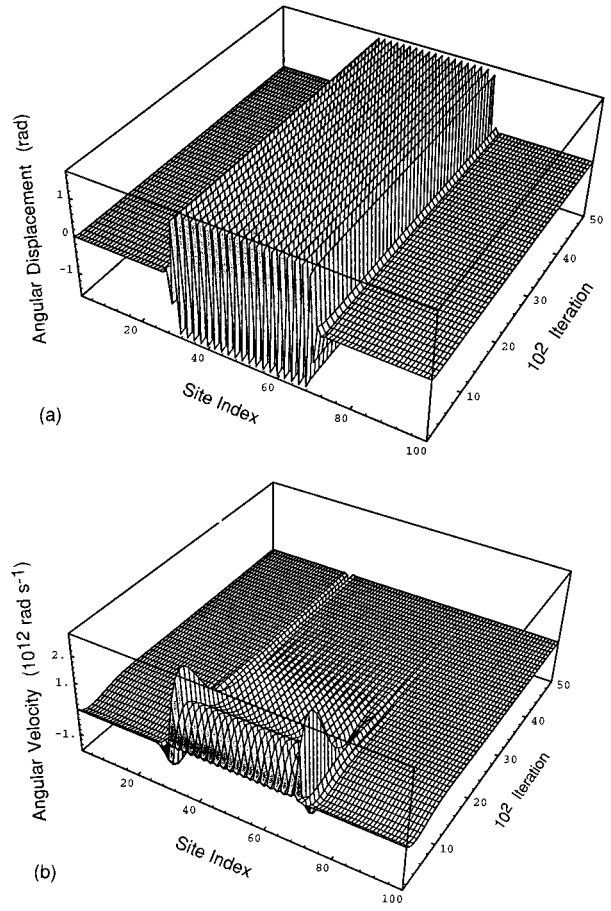

FIG. 5. Relaxation of lattice after insertion of defect pair with two-site characteristic width at sites 30 and 70 of 100-site lattice. In (a) and (b) the angular displacement and angular velocity, respectively, are shown over 5 ps (5000 iterations).

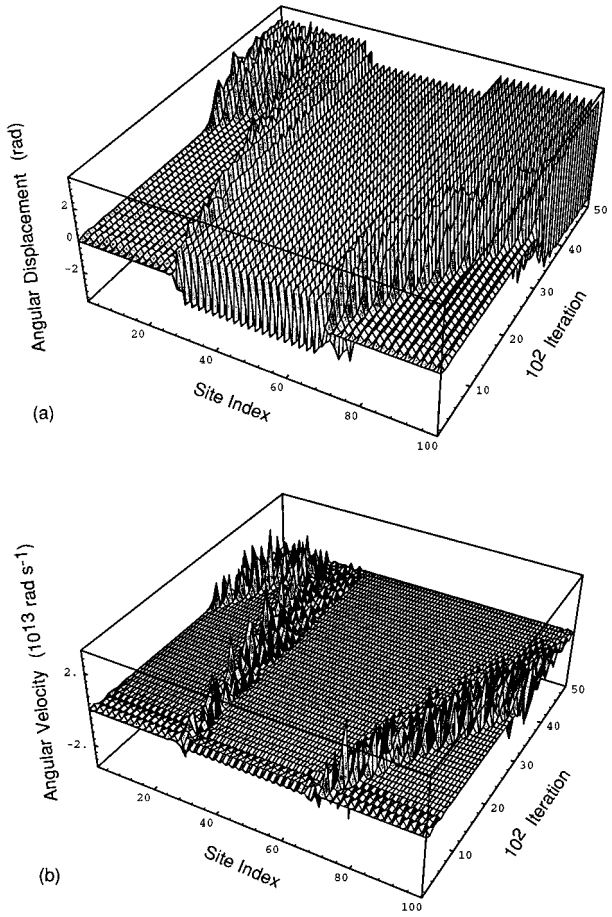

FIG. 6. Angular displacement and angular velocity, respectively, of sites accompanying defect motion in a field of 436 kV/cm, with dielectric screening of 100. In (a) and (b) the rightmost (positively charged) defect begins to move in the field direction, the leftmost (negative) defect against it, until collision and recombination occur. Each panel represents 5 ps (5000 iterations).

would, under the external field, simply ''spread'' outward to the ends of the chain. We note, however, that with the exception of a few sites, the angular displacement over the length of the chain in this final configuration *does* correspond essentially to a single phase; the $\pm 90°$ and $\pm 180°$ phases denote identical sequences of physical site orientations, except that the orientations of the odd sites in one phase correspond to those of the even sites in the other phase. Therefore, adjacent sites near site 30 and site 70—the initial defect positions—have identical (rather than alternating) orientations, one site corresponding to a 90° displacement and the next to 180°. We note that Tsironis and Pnevmatikos have indicated that interconversion of defect pairs (from, for instance, orientational to ionic) upon collision is possible for some collision speeds.[15] It is possible that if both ionic and orientational defects were incorporated in our present model, we might have observed a conversion from orientational to ionic defects upon collision. It is also possible that if the rotational displacement were followed long enough in time, it might eventually damp out to a single $\pm 90°$ phase, though this seems unlikely.

Defect motion under a range of different electric field values and screening constants was investigated. With a screening constant of one and damping of 10^{-14} eV s, no defect motion was seen at fields below 18 MV/cm; for fields between 18 and 47 MV/cm, positive defect motion only was observed. Only at fields above 47 MV/cm did motion of both defects occur. With a screening of 100, a threshold electric field of $\sim$436 kV/cm was necessary to see motion of both positive and negative defects, as shown in Fig. 6. We note that dielectric breakdown occurs for most insulators[23] in the range 10^1–10^4 kV/cm; therefore if the screening constant of one were applicable, it is doubtful that defect motion could occur.

Calculated velocities and mobilities as a function of external field, with screening factors of 50 and 100, are listed in Table I. The data of Table I for positive defects are also plotted in Figs. 7 and 8. We note that while velocity of the positive defect increases as we increase the electric field, the mobility decreases slightly with increasing field. It might be thought that the mobility decrease is due to some extent to chain length effects; that is, the positive defect may not have reached its terminal velocity, which would have been higher than that reported in Table I, before collision with the other defect. Therefore in a longer chain, mobility might have been more nearly constant over the range of fields. As a check of this possibility, we performed calculations with a defect pair, again initially centered on sites 30 and 70, on a 200-site

TABLE I. (a) Defect saturation velocity and mobility for various electric-field values and screening of 100. Note that for fields above 436 kV/cm, the negative defect moves much more slowly than the positive defect. (b) Defect saturation velocity and mobility for various electric-field values and screening of 50. Quoted values of velocities are the result of a fit by eye to density plots of lattice displacement versus site and iteration number.

Electric field (kV/cm)	Velocity (cm/s)$\times 10^5$	Mobility (cm^2/V s)
	(a)	
182	1.65	0.91
236	1.79	0.76
273	1.96	0.72
327	2.17	0.66
364	2.36	0.65
400	2.43	0.61
436	2.58 (positive defect)	0.59 (positive defect)
	0.96 (negative defect)	0.22 (negative defect)
491	2.84 (positive defect)	0.58 (positive defect)
	0.97 (negative defect)	0.20 (negative defect)
509	2.84 (positive defect)	0.56 (positive defect)
	0.94 (negative defect)	0.19 (negative defect)
	(b)	
473	2.17	0.46
545	2.43	0.45
636	2.66	0.42
727	3.17	0.44
909	3.59 (positive defect)	0.39 (positive defect)
	1.00 (negative defect)	0.11 (negative defect)

chain; the resulting positive defect mobility was unchanged from its value on the 100-site chain.

Our calculated values for positive defect mobility vary with field from 0.46 to 0.39 cm^2/V s for screening of 50; these values fall within the range of 0.1–0.5 cm^2/V s, as reported by Eigen and De Maeyer[6] for the positive defect. Screening of 100 results in a range of 0.91 to 0.56 cm^2/V s for positive defect mobility. For the negative defect, no motion, as mentioned above, was seen at fields below 436 kV/cm with a screening of 100; at this field value, the ratio of positive to negative defect mobility was 2.68, somewhat outside the range of 10–100 observed by Eigen and De Maeyer.[6]

IV. CONCLUSIONS

We have explored the formation and propagation of orientational defects on a hydrogen-bonded chain, from the point of view of both short-chain quantum-chemical calculations and longer-chain calculations based on an extended tight-binding model. In summary, our results from Hartree-Fock quantum-chemical calculations indicate that the single-chain barrier to rotations, 0.12 eV/site, is much smaller than the hopping barrier, 1.51 eV/site (calculated at UHF level with 6-31G* basis). This is in disagreement with the supposition of some that the barrier to rotation is larger. Our barrier heights for rotation were quite comparable from either the quantum chemistry calculations on a five-site chain or the longer-chain model (with a dielectric screening of one). Also, the rotational barrier was not much affected by variation in basis set, addition of correlation corrections, or the presence of an additional parallel hydrogen-bonded chain. An important point to note is that instead of using a phenomenological double well potential in our longer-chain model, we generated the double well by superposition of core-core repulsion energies and the sum over the one-electron eigenvalues of the occupied electronic states.

In the past, the continuum approximation has been widely used in the analysis of the proton transport mechanism in hydrogen-bonded chains; the present work indicates that a discrete model may be more suitable for studying proton transport in these chains, since the stable orientational defects in the proton displacement pattern are very short ($\sim$two sites long). Under a uniform applied electric field, these (charged) defects did propagate through the lattice. In order to see motion in physically reasonable fields we had to use a large screening factor, which reduces barrier height. Since our calculated barrier height with a screening of one agrees closely with that obtained from the quantum-chemical calculations, one possible conclusion is that coherent orientational defect motion is not in fact physically feasible. However, we note that the double-well potential calculated on the basis of simultaneous rotation of all sites is not in fact the potential seen by a proton in any situation *other* than simultaneous rotation (no double-well potential, for instance, exists for rotation of a single site). The range of our calculated mobilities for the positive orientational defect agrees very well with experimental values available in the literature.[6] The ratio of

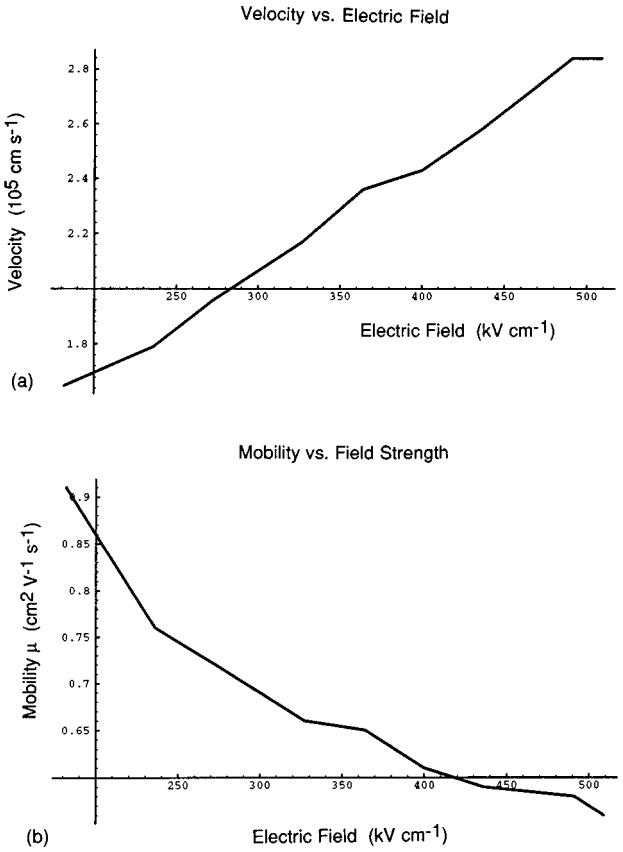

FIG. 7. Velocity (a) and mobility (b) versus electric field for the positive orientational defect, with a dielectric constant of 100.

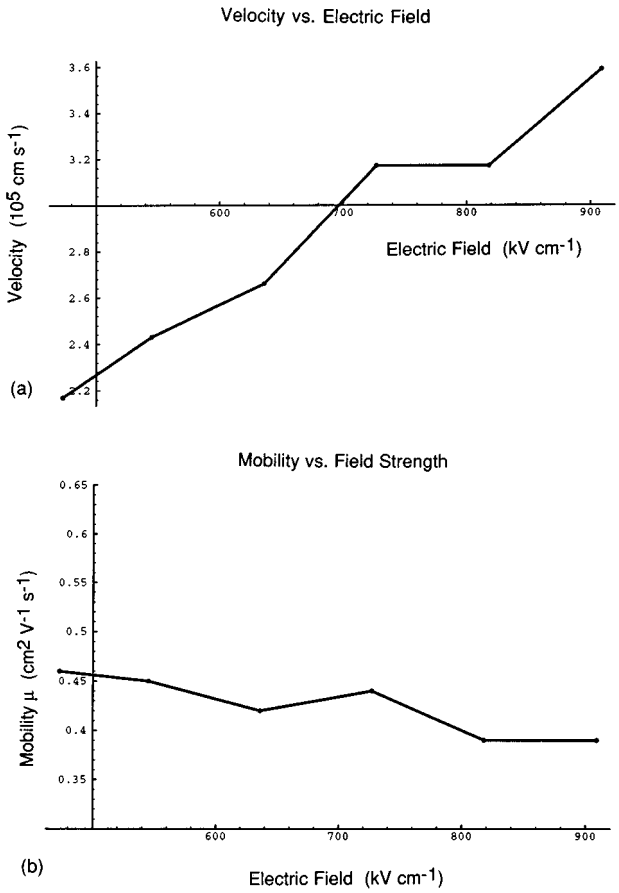

FIG. 8. Velocity (a) and mobility (b) versus electric field for the positive orientational defect, with a dielectric constant of 50.

positive defect mobility to negative defect mobility, 2.68 for a field value of 436 kV/cm and screening of 100, is in accordance with Eigen and De Maeyer's conclusion[6] that the negative defect mobility is much smaller than that of the positive defect.

Obviously, our model presents a rather simplified picture of the physical situation in a hydrogen-bonded chain. Our approach can be made more realistic in many ways. If, for instance, ionic defects, along with rotational defects, were incorporated in our model, the complete proton transfer mechanism in the physical chain could be represented. Temperature and pressure effects could also be included. There are, in addition, some indications that the defect's effective mass[24] may be less than the mass of the proton. Therefore, it may be advisable to incorporate a quantum treatment of the protonic sublattice. Nonetheless, the present treatment represents, to our knowledge, the first dynamical model of the orientational defects to incorporate a quantum-mechanical, rather than phenomenological, treatment of the electronic system of the hydrogen-bonded chain.

ACKNOWLEDGMENTS

This work has been supported by Grant No. 003656-073 from the Texas Advanced Research Program. The authors would like to acknowledge valuable discussions with G.P. Tsironis and D.K. Campbell.

[1] See, for example, *Proton Transport in Hydrogen Bonded Systems*, edited by T. Bountis (Plenum, New York, 1992), and references therein.

[2] R. W. Jansen, R. Bertoncini, D. A. Pinnick, A. I. Katz, R. C. Hanson, O. F. Sankey, and M. O'Keeffe, Phys. Rev. B **35**, 9830 (1987).

[3] M. Springborg, Phys. Rev. Lett. **59**, 2287 (1987); Phys. Rev. B **38**, 1483 (1988).

[4] E. Krauss, Phys. Rev. B **43**, 7729 (1991).

[5] P. V. Hobbs, *Ice Physics* (Clarendon, Oxford, 1974).

[6] M. Eigen and L. De Maeyer, Proc. R. Soc. London **247A**, 505 (1958).

[7] N. Bjerrum, Science **115**, 385 (1952).

[8] J. H. Weiner and A. Askar, Nature (London) **226**, 842 (1970).

[9] V. Ya. Antonchenko, A. S. Davydov, and A. V. Zolotariuk, Phys. Status Solidi B **115**, 631 (1983).

[10] E. W. Laedke, K. H. Spatschek, M. Wilkens, Jr., and A. V. Zolotariuk, Phys. Rev. A **32**, 1161 (1985).

[11] M. Peyrard, St. Pnevmatikos, and N. Flytzanis, Phys. Rev. A **36**, 903 (1987).

[12] E. S. Nylund and G. P. Tsironis, Phys. Rev. Lett. **66**, 1886 (1991).
[13] E. Nylund, K. Lindenberg, and G. Tsironis, J. Stat. Phys. **70**, 163 (1993).
[14] S. Pnevmatikos, Phys. Rev. Lett. **60**, 1534 (1988).
[15] G. P. Tsironis and S. Pnevmatikos, Phys. Rev. B **39**, 7161 (1989).
[16] St. Pnevmatikos, G. P. Tsironis, and A. V. Zolotaryuk, J. Mol. Liq. **41**, 85 (1989).
[17] S. N. Pnevmatikos and G. P. Tsironis, J. Phys. (Paris) Colloq. **50**, C3-3 (1989).
[18] J. D. Bernal and R. H. Fowler, J. Chem. Phys. **1**, 515 (1933).
[19] GAUSSIAN 92, Revision C, M. J. Frisch, G. W. Trucks, M. Head-Gordon, P. M. W. Gill, M. W. Wong, J. B. Foresman, B. G. Johnson, H. B. Schlegel, M. A. Robb, E. S. Replogle, R. Gomperts, J. L. Andres, K. Raghavachari, J. S. Binkley, C. Gonzalez, R. L. Martin, D. J. Fox, D. J. Defrees, J. Baker, J. J. P. Stewart, and J. A. Pople, Gaussian, Inc., Pittsburgh, PA, 1992.
[20] W. J. Hehre, L. Random, P. v.R. Schleyer, and J. A. Pople, *Ab Initio Molecular Orbital Theory* (Wiley, New York, 1992).
[21] C. Lee, D. Vanderbilt, K. Laasonen, R. Car, and M. Parrinello, Phys. Rev. B **47**, 4863 (1993).
[22] W. Press, S. A. Teukolsky, W. T. Vetterling, and B. P. Flannery, *Numerical Recipes: The Art of Scientific Computing* (Cambridge University Press, Cambridge, 1992).
[23] *American Institute of Physics Handbook*, 3rd ed., edited by D. E. Gray (McGraw Hill, New York, 1972).
[24] G. P. Tsironis, in *Non Linear Excitations in Biomolecules*, edited by M. Peyrard (Springer, Berlin, 1995).